

1 **Insulin-AKT1-YBX1 Regulation of ANGPTL8 Promote Lipogenesis in**  
2 **Obstructive Sleep Apnea-Associated Dyslipidemia**

3 Yuenan Liu<sup>a,f</sup>, Haolin Yuan<sup>a,f</sup>, Anzhao Wang<sup>a,f</sup>, Shengming Wang<sup>a</sup>, Xu Xu<sup>a</sup>, Junhui Hu<sup>a</sup>,  
4 Jinhong Shen<sup>a</sup>, Yiming Hu<sup>a</sup>, Xinyi Li<sup>a</sup>, Niannian Li<sup>a</sup>, Zhenfei Gao<sup>a</sup>, Xiaoxu Zhang<sup>a</sup>,  
5 Xiaoman Zhang<sup>a</sup>, Yupu Liu, Huajun Xu<sup>a</sup>, Hongliang Yi<sup>a</sup>, Jian Guan<sup>a,\*</sup>, Zhiqiang Li<sup>d,e,\*</sup>,  
6 Yongxu Zhao<sup>b,c,\*</sup>, Shankai Yin<sup>a,\*</sup>, Feng Liu<sup>a,\*</sup>

7 **Affiliations**

8 <sup>a</sup> Department of Otolaryngology Head and Neck Surgery, Shanghai Key Laboratory of  
9 Sleep Disordered Breathing, Otolaryngological Institute of Shanghai Jiao Tong  
10 University, Shanghai Jiao Tong University School of Medicine Affiliated Sixth  
11 People's Hospital, Shanghai 200233, China.

12 <sup>b</sup> Shanghai Institute of Materia Medica, Chinese Academy of Sciences, Shanghai  
13 201203, China.

14 <sup>c</sup> Shandong Laboratory of Yantai Drug Discovery, Bohai Rim Advanced Research  
15 Institute for Drug Discovery, Shandong 264117, China.

16 <sup>d</sup> The Affiliated Hospital of Qingdao University & The Biomedical Sciences Institute  
17 of Qingdao University (Qingdao Branch of SJTU Bio-X Institutes), Qingdao  
18 University, Qingdao, 266003, China.

19 <sup>e</sup> Bio-X Institutes, Key Laboratory for the Genetics of Developmental and  
20 Neuropsychiatric Disorders (Ministry of Education), the Collaborative Innovation  
21 Center for Brain Science, Shanghai Jiao Tong University, Shanghai, 200030, China.

22 <sup>f</sup> These authors contributed equally to this work.

23 \* Corresponding authors.

24 E-mail addresses: [guanjian0606@sina.com](mailto:guanjian0606@sina.com) (J Guan), [lizqsjtu@163.com](mailto:lizqsjtu@163.com) (Z Li),  
25 [zhaoyongxu@simm.ac.cn](mailto:zhaoyongxu@simm.ac.cn) (Y Zhao), [skyin@sjtu.edu.cn](mailto:skyin@sjtu.edu.cn) (S Yin), [liufeng@sibs.ac.cn](mailto:liufeng@sibs.ac.cn) (F

27 Leading contact: [liufeng@sibs.ac.cn](mailto:liufeng@sibs.ac.cn) ( F Liu)

28

29 **Abstract**

30 **Dyslipidemia is a hallmark of obstructive sleep apnea (OSA)-induced metabolic**  
31 **syndrome, yet the mechanisms remain poorly understood. We conducted a**  
32 **genome-wide association study on lipid traits in the OSA cohorts, identifying the**  
33 **SNP rs3745683 in *ANGPTL8*, significantly associated with reductions in multiple**  
34 **lipid traits. *ANGPTL8*, an essential lipogenic hormone and potential therapeutic**  
35 **target for metabolic syndrome, showed elevated expression in OSA patients**  
36 **compared to healthy controls, strongly correlated with increased insulin levels.**  
37 **Notably, *ANGPTL8* expression can be upregulated by insulin stimulation,**  
38 **indicating it as an insulin-responsive hormone regulating dyslipidemia in OSA.**  
39 **Mechanistically, SNP rs3745683 attenuated *ANGPTL8* transcription by**  
40 **inhibiting its binding to transcription factor YBX1. Insulin prompted AKT1 to**  
41 **phosphorylate YBX1 at Ser102, facilitating YBX1's nuclear translocation and**  
42 **subsequent regulation of *ANGPTL8* expression and lipid synthesis. Specific**  
43 **knockdown of YBX1 in mouse liver confirmed its necessity for *ANGPTL8***  
44 **expression and hepatic lipid synthesis in vivo. Our findings highlight *ANGPTL8***  
45 **as a critical regulator of dyslipidemia in OSA patients, offering a promising**  
46 **therapeutic avenue for managing metabolic syndrome in OSA.**

47 **Keywords** *ANGPTL8*, dyslipidemia, GWAS, obstructive sleep apnea, YBX1

48

49

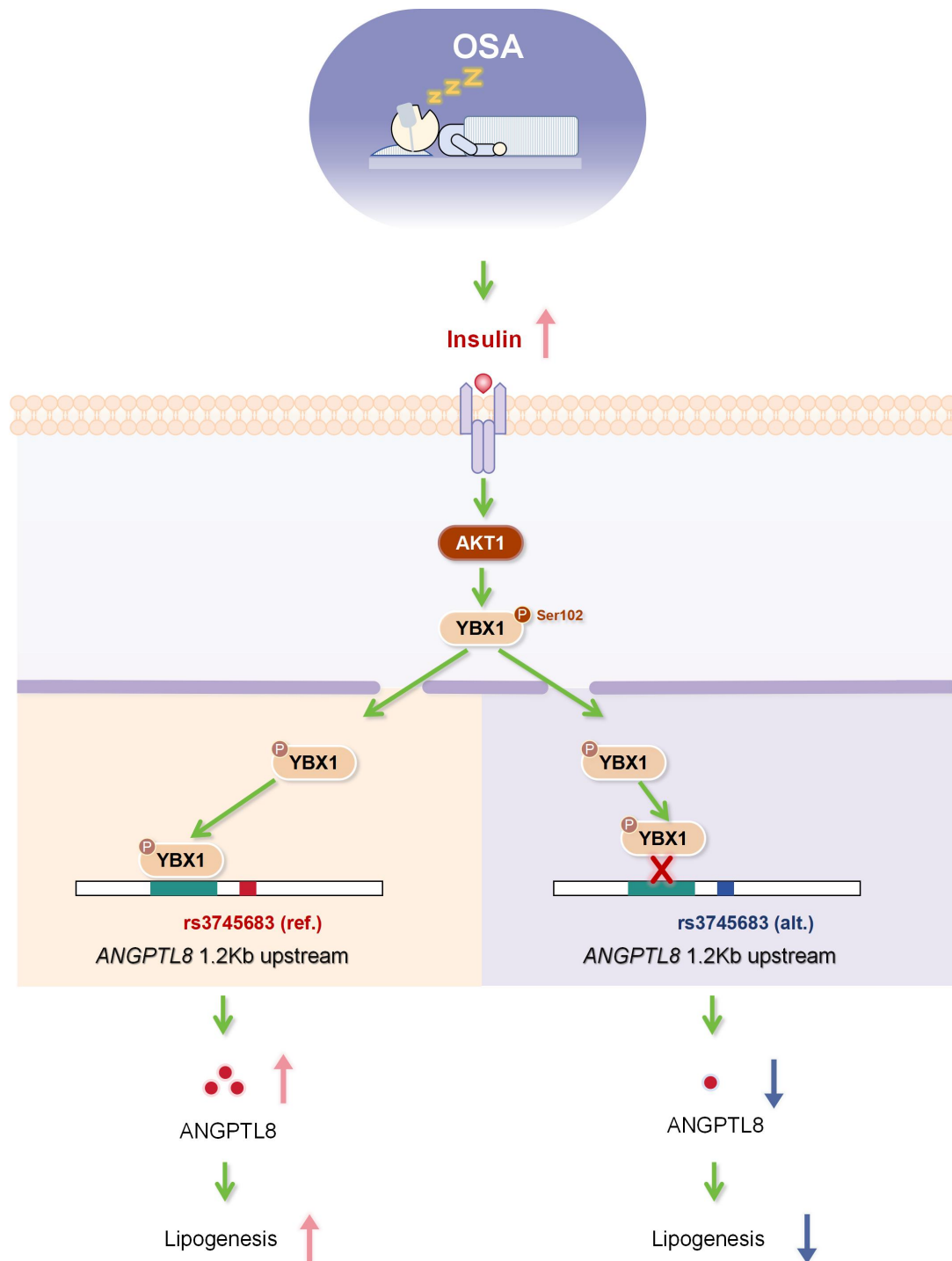
50

51

52

53 | **Synopsis**

54



55

56 ANGPTL8 serves as a crucial regulator of lipid metabolism abnormalities in  
57 obstructive sleep apnea. OSA elevates insulin levels, which, through the AKT1-YBX1  
58 signaling pathway, interact with genetic variants in OSA patients to influence the

59 expression of ANGPTL8 and lipid synthesis.

60 ◆ The genetic variant rs3745683 in ANGPTL8 is associated with lipid profiles in  
61 patients with obstructive sleep apnea (OSA).

62 ◆ Elevated insulin levels observed in OSA patients enhance the expression of  
63 ANGPTL8 and lipid synthesis.

64 ◆ Insulin signaling facilitates the phosphorylation and nuclear translocation of  
65 YBX1, which interacts with rs3745683, collectively influencing the expression of  
66 ANGPTL8 and lipid biosynthesis.

## 67 **The paper explained**

### 68 **Problem**

69 Obstructive sleep apnea (OSA) increases the risk of dyslipidemia, which can lead to  
70 serious cardiovascular complications. However, the underlying mechanisms remain  
71 unclear.

### 72 **Results**

73 The GWAS identified a single nucleotide polymorphism (SNP), rs3745683, in  
74 ANGPTL8, which is significantly associated with decreases in multiple lipid traits in  
75 the OSA cohort. Deficiency of ANGPTL8 led to impaired lipogenesis in hepatocytes  
76 and adipocytes. Rs3745683 attenuated ANGPTL8 transcription by suppressing the  
77 binding of its proximal element to the upstream transcription factor YBX1. OSA  
78 patients exhibited elevated insulin levels, which were highly correlated with increased  
79 ANGPTL8 expression. In response to insulin, AKT1 interacted with YBX1 and  
80 phosphorylated it at Ser102, promoting its nuclear translocation and subsequent  
81 regulation of ANGPTL8 expression and lipid synthesis. Specific knockdown of YBX1  
82 in mouse liver confirmed that YBX1 is required for ANGPTL8 expression and hepatic  
83 lipid synthesis in vivo.

### 84 **Impact**

85 Our findings highlight ANGPTL8 as a critical regulator of dyslipidemia in OSA  
86 patients. We demonstrated that the insulin-AKT1-YBX1 signaling pathway, in  
87 conjunction with genetic variations, modulates ANGPTL8 expression and lipid  
88 metabolism in OSA-associated dyslipidemia and offered a promising therapeutic  
89 avenue for managing metabolic syndrome in OSA patients.

90

91

## 92 **Introduction**

93 Metabolic syndrome (MS) is distinguished by the co-occurrence of numerous  
94 metabolic abnormalities, including central obesity, hyperglycemia (comprising  
95 impaired glucose tolerance and diabetes), hyperinsulinemia, hypertension, and  
96 dyslipidemia. It constitutes a significant predisposition to cardiovascular disease  
97 (CVD) [1]. Substantial research consistently underscores that individuals afflicted  
98 with obstructive sleep apnea (OSA), a prevalent sleep-disordered breathing disorder  
99 characterized by chronic and intermittent hypoxia as well as enduring sleep  
100 deprivation, exhibit a notably heightened susceptibility to developing MS when  
101 juxtaposed with the general populace [2-4]. Furthermore, there is compelling evidence  
102 that OSA considerably augments the risk of manifesting a spectrum of comorbidities  
103 associated with metabolic syndrome, while concurrently contributing to escalated  
104 all-cause mortality [3, 5]. Nonetheless, the exact molecular underpinnings governing  
105 these relationships remain elusive and necessitate further scholarly inquiry.

106 Alterations in endocrine hormones represent pivotal factors in the genesis of  
107 metabolic syndrome. Angiopoietin like 8 (ANGPTL8), a hepatic and adipose  
108 tissue-secreted protein hormone with evolutionary conservation across multiple  
109 species, plays an indispensable role in metabolic regulation [6]. A growing body of  
110 research, founded on clinical data and murine models, substantiates the central role of  
111 ANGPTL8 as a responsive agent in the domains of food intake, estrogen, and insulin  
112 signaling within the intricate terrain of glycemic and lipid metabolism [7, 8]. This

113 multifaceted protein exhibits close associations with a spectrum of human conditions,  
114 including dyslipidemia [9], obesity [10], metabolic syndrome [10, 11], cardiovascular  
115 maladies [12], type 2 diabetes mellitus (T2DM) [13], and obstructive sleep apnea [14,  
116 15]. In its current sphere of investigation, *ANGPTL8*, operating as an endocrine  
117 hormone, orchestrates a symphony of effects by modulating the physiological  
118 functions of diverse organs and tissues throughout the body, including the liver [16,  
119 17], pancreas [18], muscles [19], and adipose tissue [19, 20]. Collectively, these  
120 studies contribute to the intricate tapestry of metabolic processes that oversee  
121 glycemic and lipid regulation.

122 In the human context, the regulation of metabolism and the etiology of metabolic  
123 diseases frequently bear a discernible genetic signature [21-24]. Comprehensive  
124 human genetic inquiries, encompassing whole-genome association analyses,  
125 irrefutably substantiate the intimate interconnection between *ANGPTL8* and a gamut  
126 of metabolic disorders [25-28]. Moreover, these investigations unveil a multitude of  
127 genetic loci within *ANGPTL8* intricately intertwined with aberrations in lipid  
128 metabolism [25-28]. Among these loci, rs2278426 (C>T), a non-synonymous single  
129 nucleotide polymorphism (SNP) within *ANGPTL8*, correlates with decreased serum  
130 levels of low-density lipoprotein cholesterol (LDL-C) and high-density lipoprotein  
131 cholesterol (HDL-C) in African Americans and Hispanics [29]. Another SNP,  
132 rs3745683 (G>A), situated in the *ANGPTL8* promoter region, has been associated  
133 with serum HDL-C levels [26]. However, past investigations have provided limited  
134 insights into how genetic variations in *ANGPTL8* interact with physiological or  
135 pathological factors, thereby elucidating the specific mechanisms by which it  
136 modulates the biological functions governing glucose and lipid metabolism.

137 In our antecedent study, leveraging the Shanghai Sleep Health Study (SSHS) cohort,  
138 comprising 5,438 PSG-confirmed OSA patients and 15,152 non-OSA healthy controls,  
139 we conducted an extensive genome-wide association study (GWAS). Within this  
140 ambit, we identified 18 significant loci linked to susceptibility to OSA and  
141 OSA-related quantitative traits, encompassing parameters such as sleep architecture,

142 respiratory events, and oxygen saturation [30]. Concurrently, within the purview of  
143 this research undertaking, we conducted a GWAS analysis on the metabolic profiles  
144 of the same cohort. This analysis unveiled a notable correlation between a SNP  
145 rs3745683(G>A) in the *ANGPTL8* promoter region and a diverse array of metabolic  
146 traits, including but not limited to HDL-C, TC, and ApoA. In delving further into the  
147 transcriptional regulatory mechanisms governing rs3745683(G>A), we unveiled the  
148 intricate molecular apparatus modulating *ANGPTL8* expression. Specifically, our  
149 investigations illuminated the role of the insulin-AKT1 signaling pathway in  
150 modulating *ANGPTL8* expression through the orchestration of nuclear translocation  
151 of the transcription factor YBX1. We unveiled a potential regulatory pathway  
152 underlying the dysregulation of lipid metabolism caused by OSA.

## 153 **Materials and Methods**

### 154 **Clinical cohort**

155 Individuals enrolled in this study were from SSHS cohort. The SSHS study adheres to  
156 the Declaration of Helsinki and is registered in the Chinese Clinical Trial Registry  
157 (ChiCTR1900025714). It has received ethical approval from the Ethics Committee of  
158 Shanghai Sixth People's Hospital (Approval No.2021-KY-76), and the collection and  
159 preservation of genetic samples have been authorized by the China Human Genetic  
160 Resources Management Office (Approval No. 2022-BC0010).

161 The cohort consists of 5,438 OSA cases and 15,152 controls from Han Chinese. The  
162 individuals, genotyping and statistical analysis strategies were described in detail in  
163 our previous study [30]. Next, subjects from SSHS in this study, were screened  
164 according to the following exclusion criteria. (i) age less than 18 years old; (ii) history  
165 of OSA treatment; (iii) history of metabolic disorders treatment (i.e., hyperlipemia,  
166 T2MD); (iv) cardiovascular disease; (v) unavailable standard polysomnography data.  
167 A total 4,692 participants were ultimately analyzed in this study.

### 168 **Animal studies**

169 All animal studies were supervised and approved by the Animal Care Committee of

170 Shanghai Six People's Hospital affiliated to Shanghai Jiao Tong University School of  
171 Medicine, and the animal welfare ethics acceptance number is No:2019-0237.  
172 Four-week-old C57BL/6N SPF male mice were purchased from GemPharmatech  
173 (China), The mice were randomly allocated to the experimental group or control  
174 group, and kept at humidity environment with free access to food and water in a  
175 standard light-dark cycle.

176 Before the adeno-associated virus (AAV) construction, the target sequence used  
177 against mouse *Ybx1* was screened from three candidates in the primary hepatocyte.  
178 AAV2/8 carrying mouse *Ybx1*-shRNA (AAV2/8-TBG-*Ybx1*-shRNA) and the control  
179 vectors (AAV2/8-TBG-*EV*) were constructed, amplified, and purified by Obio  
180 Technology (China). The target sequence used against mouse *Ybx1* was as follows:  
181 5'-CCACGCAATTACCAGCAAAA-3'. AAV diluted in saline and injected via the tail  
182 vein of mice ( $2 \times 10^{11}$  vg per mouse). Three weeks later, immunoblotting or RT-qPCR  
183 were performed to examine the expression levels of *Ybx1* and *Angptl8* in mice livers.  
184 Then, the rest mice were fed with high fat-diet (HFD, 60% fat caloric content,  
185 Research Diets, D12492) and the body weights and food intakes were measured  
186 weekly. For 12 weeks of HFD feeding, we performed GTT on these mice. For 16  
187 weeks of HFD feeding, mice were sacrificed under fasting conditions, plasm, adipose  
188 and liver of mice were collected for subsequent examination.

## 189 **Cellular and Molecular Studies**

190 Genetic manipulation and metabolic measurement in human and mouse liver cell lines,  
191 as well as mouse adipocyte precursor cells, were used to investigate the role of the  
192 indicated genes in lipid metabolism. Luciferase reporter assays, CUT & Tag, DNA  
193 pull-down assays, and subsequent mass spectrometry were employed to study the  
194 transcriptional regulatory capacity of the indicated SNP and its underlying  
195 mechanisms. Quantitative PCR and Western blot analyses were performed to assess  
196 gene expression at the mRNA and protein levels. Detailed information on the  
197 materials and protocols used in the aforementioned studies is provided in the  
198 Supplementary Materials.



199 **Statistics**

200 The clinical statistical analyses were performed using SPSS 26.0 software (IBM Corp.,  
201 Armonk, NY, United States). The normally distributed data are presented as the means  
202 and standard deviation; skewed data are presented as the median (IQR), and  
203 categorical data are presented as the number (percentage). Differences in the baseline  
204 characteristics among different OSA severity degree groups were examined using  
205 one-way analysis of variance (ANOVA), non-parametric Kruskal–Wallis H test, or  $\chi^2$   
206 tests according to the type of data distribution. Baseline characteristics also tested by  
207 the polynomial linear trend test for continuous variables and the linear-by-linear  
208 association test for dichotomous variables.

209 For GWAS of OSA-related traits, the quantitative phenotypic variables were analyzed  
210 by linear regression under an additive genetic model after adjusting for age, sex,  
211 cigarette consumption, and alcohol consumption. Logistic regression analyses were  
212 performed to evaluate the relationship between polymorphisms and categorical  
213 variables.

214 For other statistical analysis, the results were presented as the mean  $\pm$  SEM. Statistical  
215 significance among multiple groups was analyzed by one-way ANOVA, followed by  
216 Student's t test using Prism 8 (GraphPad Software, Inc.) to compare the results  
217 between two groups.  $P < 0.05$  was considered to be statistically significant.

218 **Results**

219 **GWAS revealed novel genetic loci associated with serum lipid levels in OSA**  
220 **patients**

221 To better elucidate the genetic factors underlying metabolic abnormalities in  
222 individuals with OSA, we performed a GWAS using SSHS cohort focusing on four  
223 serum lipid traits including total cholesterol (CHOL), triglyceride (TRIG),  
224 low-density lipoprotein cholesterol (LDL-C) and high-density lipoprotein cholesterol  
225 (HDL-C), and identified 18 genome-wide significant loci ( $p < 5 \times 10^{-8}$ ) (Fig. 1a-1d).

226 Among them, 2 loci (rs3832016, and rs80246393) were identified for CHOL; 9 loci  
227 (rs80266524, rs57539228, rs117362525, rs151299191, rs147511495, rs651821,  
228 rs34528262, rs79929907, and rs483082) were identified for TRIG; 2 loci (rs12740374,  
229 and rs72654473) were identified for LDL-C; and the rest 5 loci (rs115849089,  
230 rs651821, rs12149545, rs3786247, and rs3745683) were identified for HDL-C ([Table](#)  
231 [1](#)).

232 Further analysis revealed no significant correlations between these loci and OSA  
233 respiratory events, blood oxygen saturation, or sleep architectures ([Supplementary Fig.](#)  
234 [S1a - S1b](#)). However, several loci demonstrated extensive associations with various  
235 metabolic traits. Notably, rs72654473 was closely associated with LDL-C, ApoB, and  
236 ApoE levels, while rs651821 showed strong associations with TRIG, HDL-C, and  
237 ApoE levels ([Fig. 1e](#)). The annotation and expression quantitative trait locus (eQTL)  
238 analysis of the 18 SNPs revealed that several loci or risk genes are widely  
239 characterized in several other GWAS of lipid traits, including *APOA5* (rs651821),  
240 *APOE* (rs72654473), *APOC1* (rs483082), *CELSR2* (rs3832016, rs12740374), *CETP*  
241 (rs12149545) and *LIPG* (rs3786247). Furthermore, eight SNPs, including the  
242 CHOL-associated SNP (rs80246393) and TRIG-associated SNPs (rs80266524,  
243 rs57539228, rs117362525, rs147511495, rs151299191, rs34528262, and rs79929907),  
244 along with their affected genes, have not been previously reported in relation to lipid  
245 metabolism ([Supplementary Table S1](#)).

246 The annotation analysis showed that rs3745683 is located in the upstream region of  
247 *ANGPTL8* gene ([Fig. 1f](#)). Clinical data reveal elevated levels of ANGPTL8  
248 expression in the serum of OSA patients ([Fig. 1g, 1h](#)), and previous studies has also  
249 suggested that ANGPTL8 expression can serve as an indicator of OSA improvement  
250 following weight loss surgery [[15](#)], Consequently, we have selected rs3745683 for our  
251 subsequent investigations.

252 A subpopulation of 4,692 individuals from SSHS cohort, comprising 658 healthy  
253 controls, 258 Mild OSA, 969 Moderate OSA, 2,852 Severe OSA, were analyze to  
254 further validate the association of rs3745683 and serum lipid levels ([Supplementary](#)

255 [Table S2](#)). The results revealed a significant association between the rs3745683 (G>A)  
256 variant and lower serum HDL-C, CHOL, ApoA and non HDL-C levels, which is a  
257 well characterized risk factor for CVD ([Fig. 1i-1l](#), [Supplementary Fig. S1g, S1h](#)).  
258 Stratifying by OSA severity and adjusting for age, gender, cigarette consumption, and  
259 alcohol consumption, multiple linear regression analysis under an additive model  
260 revealed a significant inverse association ( $p < 0.05$ ) between the rs3745683 and serum  
261 levels of HDL-C, CHOL, and ApoA across the three groups and the total population  
262 ([Fig. 1m, 1n](#), [Supplementary Table S3](#)). Furthermore, compared to the non OSA group  
263 ( $\beta = -0.037$ ,  $p = 0.018$ ), rs3745683 exhibited a more pronounced regulatory effect on  
264 HDL-C levels in the moderate OSA group ( $\beta = -0.044$ ,  $p = 4.21 \times 10^{-4}$ ) ([Fig. 1m](#),  
265 [Supplementary Table S3](#)). Propensity score matching analysis, which accounted for  
266 differences in sample size, confirmed that rs3745683 remained significantly  
267 associated with serum HDL-C levels in the moderate OSA group ( $p = 0.004$ ) ([Fig. 1m](#),  
268 [Supplementary Tables S4, S5](#)). In summary, data from clinical samples further  
269 validated the strong correlation between rs3745683 and lipid traits.

### 270 **Functional impact of SNP rs3745683 on transcriptional activity and its role in** 271 **modulating lipid metabolism through ANGPTL8 expression**

272 The locus annotation shows that rs3745683 is located 1,774 bp upstream of the  
273 transcription start site (TSS) of *ANGPTL8* and within the 14th intron of *DOCK6* ([Fig.](#)  
274 [2a](#)). Analysis of Ensembl data revealed its localization within an active region  
275 associated with transcriptional regulation ([Fig. 2a](#)). Furthermore, eQTL analysis from  
276 GTEx Portal Database demonstrated a significant correlation between the expression  
277 of *DOCK6* and rs3745683 in various tissues, such as Adipose\_Subcutaneous ( $\beta = 1.0$ ,  
278  $p = 1.3 \times 10^{-35}$ ), Artery\_Tibial ( $\beta = 1.2$ ,  $p = 2.8 \times 10^{-54}$ ), and Esophagus\_Muscularis ( $\beta =$   
279  $1.1$ ,  $p = 7.8 \times 10^{-36}$ ). Additionally, in Artery\_Tibial ( $\beta = -0.29$ ,  $p = 1.4 \times 10^{-3}$ ) and  
280 adipose\_naive ( $\beta = -0.56$ ,  $p = 2.1 \times 10^{-3}$ ), expression of *ANGPTL8* was also found to be  
281 associated based on Ensembl database ([Supplementary Table S6](#)). Therefore, we  
282 hypothesize that rs3745683 may influence the transcriptional activity of this  
283 chromosomal region. To address this hypothesis, we cloned DNA fragments of 1,200

284 bp containing the SNP into the 5' end of a luciferase reporter gene (Fig. 2b,  
285 Supplementary Table S7). Luciferase activity was subsequently assessed in multiple  
286 lipid metabolism-related cell lines with reference allele of rs3745683, including  
287 human hepatocytes (HepG2, LO2), mouse hepatocytes (AML12), and mouse  
288 preadipocytes (Supplementary Fig. S2a, S2b). Remarkably, the results consistently  
289 demonstrated a significant increase in luciferase activity associated with the  
290 SNP-linked DNA fragments across different cell types. Furthermore, in comparison to  
291 the reference allele construct, the alternative construct significantly decreased  
292 transcriptional activity in all four cell lines (Fig. 2c-2f). These findings provide  
293 compelling evidence supporting the notion that rs3745683 may have a functional  
294 impact on transcriptional activity in relevant cellular contexts.

295 Given the potential concurrent impact of rs3745683 on the expression of *DOCK6* and  
296 *ANGPTL8*, our investigation aimed to elucidate the key genes influenced by  
297 rs3745683 in the context of metabolic dysregulation. Previous studies have already  
298 established *ANGPTL8*, which highly expressed in liver and adipose tissue  
299 (Supplementary Fig. S3a), as a pivotal regulator of lipid metabolism. Our comparative  
300 analysis of *ANGPTL8* expression in the serum of individuals carrying different alleles  
301 of rs3745683 revealed that homozygous individuals (n=31) carrying the alternative  
302 allele (A) exhibited significantly reduced levels of *ANGPTL8* in their serum  
303 compared to both homozygous (n=39) and heterozygous individuals (n=56) with the  
304 reference allele (G) (Fig. 3a). Furthermore, CRISPR/Cas9 technology was used to  
305 conducted separate deletions of *Angptl8* in both mouse hepatocyte AML12 cells and  
306 adipocytes (Fig. 3b, 3c). Compared to wildtype control, the formation of lipid droplets  
307 and TRIG content were significantly decreased in *Angptl8*-sgRNAs transfected cells  
308 (Fig. 3d-3g), suggesting that *Angptl8* was required for triglyceride synthesis in both  
309 hepatocytes and adipocytes. Furthermore, we systematically excluded the  
310 involvement of *Dock6* deficiency in the observed TRIG synthesis changes  
311 (Supplementary Fig. S3b-S3d). As a consequence, we have substantiated that the SNP  
312 exerts its influence on lipid metabolism through the modulation of *ANGPTL8*

313 expression.

314 **Identification of transcription factors YBX1, YBX2, PCBP1, and PCBP2 that**  
315 **bound to proximal sequence of rs3745683**

316 To investigate whether rs3745683 influences the binding of adjacent DNA fragments  
317 to transcription factors or chromatin factors, biotin-labeled DNA probes, designed to  
318 mimic the DNA fragments associated with the SNP reference (G) and alternative (A)  
319 alleles, were synthesized at a length of 50 base pairs (bp) (Fig. 4a). Following  
320 incubation with HepG2 nuclear extracts, the resulting precipitates were subjected to  
321 streptavidin-based affinity chromatography. Subsequently, the protein bands  
322 specifically enriched in the precipitates containing the reference allele probe were  
323 subjected to mass spectrometry (MS) analysis. Through this method, we successfully  
324 identified the specific enrichment of transcription factors YBX1, YBX2, PCBP1, and  
325 PCBP2, collectively termed YYPP (Fig. 4b, 4c).

326 We further validated the affinity precipitation results by conducting experiments in  
327 HepG2, which revealed a stronger enrichment of the transcription factor YBX1,  
328 PCBP1 and PCBP2 with the reference allele probe (Fig. 4d). Previous studies have  
329 indicated YYPP as a tightly bound protein complex [31-33], and YBX1 can directly  
330 bind to DNA sequences with a binding motif represented by (5'-TGTACCATC-3')  
331 (Fig. 4f). Through sequence comparison, we identified that the proximal sequence to  
332 rs3745683 conforms to the binding motif characteristic of YBX1. Moreover, a further  
333 analysis of the upstream transcriptional regulatory sequence of mouse *Angptl8*  
334 revealed the presence of multiple YBX1 binding motifs (Fig. 4e-4g). Therefore, we  
335 hypothesize that YYPP are required for the transcriptional regulation of *ANGPTL8*  
336 expression cross species.

337 **YBX1 responds to insulin signaling and regulates *ANGPTL8* expression**

338 Intermittent hypoxia and elevated insulin levels are two pathophysiological features in  
339 individuals with OSA, therefore, we investigated whether these factors affect the  
340 expression of *ANGPTL8* through YYPP [34]. Despite the ability of hypoxia

341 stimulation to induce an increase in *ANGPTL8* expression ([Supplementary Fig. S4k](#)),  
342 the core transcription factor of hypoxia signaling, hypoxia inducible factor 1 subunit  
343 alpha (HIF1 $\alpha$ ), was not enriched in the rs3745683 DNA fragment. Furthermore, Co-IP  
344 experiments did not reveal any interaction between HIF1 $\alpha$  and YYPP ([Supplementary](#)  
345 [Fig. S4a-S4d](#)). Additionally, luciferase reporter assays demonstrated that  
346 overexpression of YYPP did not alter the transcription of HIF1 $\alpha$ -responsive reporters  
347 ([Supplementary Fig. S4e-S4h](#)). Taken together, our results indicate that hypoxia  
348 signaling does not regulate *ANGPTL8* expression through the YYPP and rs3745683.

349 Since the little effect of HIF1 $\alpha$  on *ANGPTL8* expression by rs3745683, we focus on  
350 insulin signaling. Within our OSA cohort, we observed a substantial elevation in  
351 serum insulin levels and *ANGPTL8* levels ([Fig. 1g, 1h, Fig. 5a-5b](#)). We conducted  
352 further analysis on a subpopulation of 123 individuals from the SSHS cohort to clarify  
353 the relationship between *ANGPTL8* and insulin levels. Considerate the influence of  
354 insulin resistance, we then stratified HOMA-IR into quartiles corresponding to a  
355 HOMA-IR of Q1 (n = 30, HOMA-IR < 1.39), Q2 (n = 30, 1.39  $\leq$  HOMA-IR < 2.00),  
356 Q3 (n = 32, 2.00  $\leq$  HOMA-IR < 2.83), Q4 (n = 31, HOMA-IR  $\geq$  2.83). Linear  
357 regression analysis showed a significantly positive correlation ( $R^2 = 0.1775$ ,  $p =$   
358  $0.0203$ ) between serum *ANGPTL8* and fasting insulin levels in group Q1 which  
359 performed a better insulin sensitivity compared to other groups. While, within the  
360 insulin resistance getting worse, the correlation between *ANGPTL8* and insulin level  
361 getting weak ([Fig. 5c](#)). Collectively, these results implied that insulin facilitated  
362 *ANGPTL8* expression and the decrease of sensitivity of insulin signaling pathway  
363 inhibited this progress.

364 Additionally, both preadipocytes and hepatocytes demonstrated a significant  
365 upregulation of *ANGPTL8* expression in response to insulin signaling ([Fig. 5d](#)). To  
366 investigate whether the transcription factors YYPP mediate insulin regulation of  
367 *ANGPTL8*, we utilized CRISPR/Cas9 technology to perform targeted silence of YYPP  
368 expression in preadipocytes and AML12 cells ([Fig. 5e, 5f](#)). The results unequivocally  
369 showed that the depletion of YYPP in both cell types resulted in a substantial

370 reduction in *ANGPTL8* expression and TRIG contents (Fig. 5g-5l). Consistently,  
371 overexpression of YYPP significantly increased *ANGPTL8* expression in all of four  
372 adipose and hepatic cell lines (Fig. 5m). Furthermore, luciferase reporter assays  
373 provided compelling additional evidence, supporting the notion that the loss of YYPP  
374 significantly impaired the transcriptional regulatory activity of *ANGPTL8* (Fig. 5n,  
375 5o).

376 We then examined the cellular localization of YYPP in preadipocytes. In the untreated  
377 state, PCBP1 and PCBP2 were localized in the cell nucleus, whereas YBX1 and  
378 YBX2 were predominantly found in the cytoplasm (Fig. 6a). Upon insulin stimulation,  
379 YBX1 exhibited increased expression and translocated from the cytoplasm to the  
380 nucleus (Fig. 6a-6b). To investigate the signaling mechanisms involved in insulin  
381 stimulation, we examined the downstream activation of the PI3K-AKT and ERK  
382 MAP kinase pathways [35]. We used specific inhibitors, LY294002 and PD98059, to  
383 inhibit the PI3K-AKT and ERK MAP kinase pathways, respectively. Notably,  
384 inhibition of the PI3K-AKT pathway significantly reduced the nuclear translocation  
385 of YBX1, indicating that AKT kinase activity is crucial for nuclear YBX1 expression  
386 (Fig. 6c). This finding is supported by previous studies reporting AKT-mediated  
387 phosphorylation of YBX1 at Ser102 [36].

388 To validate this, we performed immunoblot experiments, which demonstrated clear  
389 insulin-induced phosphorylation of YBX1 at the Ser102 site across different cell types.  
390 Peak phosphorylation and subsequent nuclear translocation of YBX1 were observed  
391 30 minutes after insulin treatment (Fig. 6b, 6d-6g). Furthermore, through  
392 immunoprecipitation experiments, we confirmed the protein interaction between  
393 AKT1 and YBX1, but did not observe interactions between YBX1 and AKT2 or  
394 AKT3 (Fig. 6h, Supplementary Fig. S4i, S4j). Collectively, these findings provide  
395 strong evidence that the insulin-AKT1 signaling pathway promotes the nuclear  
396 translocation of YBX1 through its phosphorylation.

397 To validate our observations, we generated two mutants of YBX1 at Ser102: the  
398 non-phosphorylatable Ser102Ala (S102A) and the phospho-mimicking Ser102Asp

399 (S102D) mutants, along with mutants at other serine residues potentially involved in  
400 phosphorylation (Fig. 7a, Supplementary Fig. S5a). Intriguingly, the S102D and  
401 S176A mutants consistently exhibited nuclear localization even in the absence of  
402 insulin stimulation (Fig. 7a, Supplementary Fig. S5a). In *Ybx1*-sgRNA transfected  
403 cells, the S102D, S176A, and S176D mutants restored the expression of *Angptl8* (Fig.  
404 7b, 7c). In wildtype adipocytes and AML12 cells, transfection with the S102D, S176A,  
405 and S176D mutants significantly increased *Angptl8* expression and led to a notable  
406 elevation of TRIG content within the cells (Fig. 7d-7g).

407 Furthermore, we employed Cleavage Under Targets and Tagmentation (CUT & Tag)  
408 and real-time quantitative PCR (RT-qPCR) using an anti-H3K27Ac antibody to assess  
409 the transcriptional activity of the rs3745683 locus proximal region. Results showed  
410 that insulin increased the enrichment of the rs3745683 locus proximal region in  
411 HepG2 cells; however, this effect was inhibited by YBX1 deficiency (Fig. 7h). Taken  
412 together, these results indicate that YBX1 is essential for *Angptl8* expression, and the  
413 phosphorylation of YBX1 at Ser102 is critical for initiating this process.

414 We also performed RNA sequencing to analyze the gene expression profiles in *Ybx1*-  
415 and *Angptl8*- deficient AML12 cells (Supplementary Fig. S5b-S5c). Compared to the  
416 control group, 4,958 genes showed significant changes in expression ( $p < 0.05$ ) in the  
417 *Ybx1*- deficient cells, and 7,982 genes were significantly differentially expressed in  
418 the *Angptl8*- deficient cells. Among these differentially expressed genes (DEGs),  
419 1,389 genes were up-regulated in both groups ( $p < 0.05$ ,  $\log_2\text{FoldChange} > 0$ ), and  
420 1,472 genes were down-regulated in both groups ( $p < 0.05$ ,  $\log_2\text{FoldChange} < 0$ ) (Fig.  
421 7i-7j). Furthermore, functional enrichment analysis revealed that these DEGs were  
422 associated with lipid metabolism-related biological processes, such as "lipid  
423 homeostasis" and "cholesterol metabolic process" (Fig. 7k, Supplementary Fig. S5d).  
424 These results indicate similar gene expression profiles in *Ybx1*- and *Angptl8*-deficient  
425 hepatocytes, strongly suggesting that *Ybx1* affects lipid metabolism by regulating  
426 *Angptl8* expression.

427 **YBX1 regulates *Angptl8* expression and lipid metabolism in mouse liver**



428 To further explore the effect on lipid metabolism of *Ybx1* *in vivo*, we therefore  
429 performed the knock-down of *Ybx1* in liver by delivering AAV2/8 containing  
430 *Ybx1*-shRNA (AAV-*Ybx1*-shRNA) in C57BL/6J male mice, achieving approximately  
431 80% specific deficiency in *Ybx1* levels in liver (Fig. 8a-8d). Consistently, we also  
432 observed about 20% and 50% decrease of *Angptl8* in mRNA level and protein level,  
433 respectively, in *Ybx1*-deficient mouse livers (Fig. 8b-8d).

434 We conducted a 16-week high-fat diet intervention on two genotypes of mice and  
435 examined their metabolic parameters. We found that the knockdown of *Ybx1* in the  
436 liver did not significantly affect the overall metabolic characteristics of the mice,  
437 including body weight, food intake, fat mass, lean mass, as well as the weights of  
438 metabolic organs including liver, inguinal white adipose tissue (iWAT), epididymal  
439 white adipose tissue (eWAT), and brown fat (Fig. 8e-8g). Additionally, under fasting  
440 conditions, there were no significant changes in serum TRIG and CHOL levels (Fig.  
441 8i-8j). Meanwhile, mice of both genotypes after 12 weeks HDF treatment performed  
442 similarly in glucose tolerance test under fasting state (Fig. 8h). However, the levels of  
443 TRIG and CHOL were significantly decreased in *Ybx1*-deficient mouse liver,  
444 suggesting that *Ybx1* is required for the lipid synthesis in livers (Fig. 8i- 8k). A further  
445 RNA-seq analysis showed the deficiency of YBX1 in mouse liver significantly  
446 decreased *Angptl8* mRNA level (log2Foldchange = -1.114,  $p = 0.002$ ). The functional  
447 enrichment analysis showed that these significantly changed DEGs were associated  
448 with nucleotide or lipid metabolism-related biological processes, such as “nucleotide  
449 metabolic process” and “negative regulation of lipid biosynthetic process” (Fig.  
450 8l-8m). These *in vivo* results showed that deficiency of *Ybx1* decreases ANGPTL8  
451 expression in both mRNA and protein levels, and further improve TRIG and CHOL  
452 accumulation in liver.

453 To further investigate whether *YBX1* and its associated cofactors are involved in the  
454 regulation of human metabolism and the occurrence of metabolic diseases, we  
455 conducted an in-depth exploration using the EBI Metabolomics-related GWAS  
456 datasets. Unfortunately, our analysis did not identify any genetic variations in *YBX1*

457 significantly associated with various metabolic traits ( $p < 5 \times 10^{-5}$ ) (Fig. 8n). However,  
458 we did observe a genome-wide significant association between the non-coding SNP  
459 rs180915454 in *YBX2* and a decrease in total cholesterol ( $\beta = -0.213$ ,  $p = 1.20 \times 10^{-70}$ )  
460 (Fig. 8o). Additionally, the missense variant rs8069533 (p. Ser63Pro) in *YBX2* showed  
461 a genome-wide significant association with an increase in total cholesterol ( $\beta = 0.011$ ,  
462  $p = 5.81 \times 10^{-18}$ ) (Fig. 8o). Also, we identified an upstream SNP rs6546568 of *PCBPI*  
463 is a genome-wide significant variant of total cholesterol ( $\beta = 0.016$ ,  $p = 2.54 \times 10^{-15}$ )  
464 (Fig. 8p). These genetic correlation data further suggest the significant involvement of  
465 *YBX1* and its associated factors in the regulation of human metabolism.

466 Collectively, our comprehensive findings shed light on the intricate molecular  
467 mechanisms involved in YBX1-mediated regulation of *ANGPTL8* expression.

## 468 Discussion

469 A large number of studies, including meta-analyses have firmly established the  
470 profound impact of OSA, not only significantly elevating the risk of adverse health  
471 outcomes but also independently serving as a predictive factor for overall and  
472 cardiovascular mortality [37]. Additionally, individuals afflicted with OSA exhibit an  
473 enhanced susceptibility to the development of dyslipidemia and insulin resistance [38].  
474 A twin study has underscored the substantial hereditary component contributing to the  
475 emergence of dyslipidemia in OSA patients [39]. Recent genetic investigations  
476 conducted within OSA populations have shed light on the role played by genetic  
477 variations, including those within the leptin receptor and ApoA5, in the manifestation  
478 of dyslipidemia among OSA patients [40, 41].

479 Nevertheless, the precise mechanisms by which OSA instigates disruptions in lipid  
480 metabolism have remained largely uncharted. Our study has brought to the forefront a  
481 noteworthy correlation between genetic variations in the endocrine hormone  
482 *ANGPTL8* and lipid irregularities in OSA patients. Moreover, we have observed a  
483 significant elevation in *ANGPTL8* levels in OSA patients, with both of OSA's  
484 pathophysiological hallmarks, intermittent hypoxia and insulin resistance,

485 contributing to an upregulation in ANGPTL8 expression. We have further elucidated  
486 how the insulin-AKT1-YBX1 pathway, by fostering the expression of ANGPTL8,  
487 subsequently amplifies lipid synthesis in the liver and adipose tissues. Our findings  
488 serve to enhance our comprehension of the molecular mechanisms through which  
489 OSA induces abnormalities in lipid metabolism.

490 Our research, conducted at both the human genetic and molecular cellular levels,  
491 unambiguously supports the pivotal role of ANGPTL8, a serum hormone, in the  
492 context of dyslipidemia in OSA. This observation aligns with the recent body of  
493 research that underscores the extensive yet highly conserved role of ANGPTL8 in  
494 metabolic regulation. ANGPTL8, a serum hormone secreted by both the liver and  
495 adipose tissues, further modulates the glycemic and lipidic processes in muscle, liver,  
496 and adipose tissues through endocrine mechanisms. Notably, recent studies by Siyu  
497 chen et al. have revealed that ANGPTL8 can interact with hepatic surface receptor  
498 PirB, thereby influencing the expression of circadian genes in hepatocytes, with  
499 implications for hepatic metabolism [42]. Moreover, multiple investigations have  
500 underscored the pivotal role of ANGPTL8 in the onset and progression of various  
501 metabolic disorders. For instance, Zongli Zhang and colleagues unveiled that  
502 ANGPTL8 exerts a promotive effect on the development of non-alcoholic fatty liver  
503 disease [16]. Targeted strategies aimed at inhibiting ANGPTL8 have already  
504 demonstrated promising effects in models of dyslipidemia in humanized mice [16].  
505 Collectively, our research also suggests that the targeted inhibition of ANGPTL8 may  
506 hold potential therapeutic value in addressing metabolic syndrome.

507 Y-box binding protein 1 (YBX1), a member of the DNA- and RNA-binding protein  
508 family, has garnered significant attention due to its involvement in malignant cell  
509 transformation, tumor aggressiveness, and its potential as a therapeutic target in  
510 cancer and inflammation [43]. Initially recognized as a DNA transcription factor for  
511 its binding to a DNA nucleotide sequence known as the Y-box  
512 (5'-CTGATTGGC/TC/TAA-3') located in gene promoters [44], YBX1 has since been  
513 attributed to a range of functions, including DNA repair, pre-mRNA splicing,

514 translation, and packaging [45]. Recent studies have unveiled YBX1's ability to  
515 influence gene expression both within and outside the context of the Y-box sequence.  
516 Notably, DNA pulldown and LC–MS analyses conducted in our study have indicated  
517 that YBX1, in concert with YBX2, PCBP1, and PCBP2, represents potential  
518 transcription factors binding to the rs3745683 region. Furthermore, the binding  
519 affinities of YBX1, PCBP1, and PCBP2 to rs3745683 (G>A) are diminished in the  
520 presence of this genetic variation.

521 Emerging research has illuminated YBX1's role not only in tumorigenesis but also in  
522 the regulation of thermogenic gene expression in adipocytes and the transformation of  
523 white adipose tissue into brown adipose tissue [46, 47]. Another study has  
524 demonstrated that YBX1 promotes brown adipogenesis and thermogenic activity  
525 through PINK1/PRKN-mediated mitophagy [48]. These findings underscore the  
526 multifaceted functions of YBX1 in adipose tissue biology. Our study, in which we  
527 employed CRISPR/Cas9 to generate TFs-deficiency adipocyte and hepatocyte cell  
528 lines, revealed that the depletion of YBX1 significantly reduced *Angptl8* expression,  
529 intracellular lipid droplets, and triglyceride content. Furthermore, our prior research  
530 has shown that serum fasting insulin levels are positively correlated with the severity  
531 of OSA [49]. Thus, it is reasonable to infer that YBX1, a responsive factor to insulin  
532 signaling, exerts regulatory control over *ANGPTL8* expression by binding to the  
533 rs3745683 region, thereby influencing adipocyte lipid metabolism in OSA.  
534 Nevertheless, it is important to note that our study is grounded mostly *in vitro*  
535 experiments, and further *in vivo* investigations are imperative for a comprehensive  
536 understanding of these mechanisms.

### 537 **CRedit authorship contribution statement**

538 Yuenan Liu: Methodology, Investigation, Formal analysis, Data analysis,  
539 Writing-original draft. Haolin Yuan: Investigation, Validation. Anzhao Wang:  
540 Investigation, Validation. Shengming Wang: Data analysis. Xu Xu: Funding  
541 acquisition, Methodology, Investigation. Junhui Hu: Investigation. Jinhong Shen:  
542 Funding acquisition, Methodology, Investigation. Yiming Hu: Funding acquisition,

543 Methodology, Investigation. Xinyi Li: Funding acquisition, Investigation. Niannian Li:  
544 Methodology, Data analysis. Zhenfei Gao: Methodology, Investigation. Xiaoxu Zhang:  
545 Investigation. Xiaoman Zhang: Investigation. Huajun Xu: Methodology. Hongliang Yi:  
546 Funding acquisition, Methodology. Jian Guan: Funding acquisition, Supervision.  
547 Zhiqiang Li: Methodology, Supervision. Yongxu Zhao: Funding acquisition,  
548 Methodology, Investigation, Supervision. Shankai Yin: Funding acquisition,  
549 Supervision, Methodology, Writing-original draft. Feng Liu: Funding acquisition,  
550 Methodology, Supervision, Writing-original draft.

### 551 **Declaration of competing interest**

552 All authors in this study declare no competing interests.

### 553 **Declaration of generative AI and AI-assisted technologies in the writing process**

554 During the preparation of this work the authors used OpenAI's tool ChatGPT in order  
555 to improve the English grammar. After using this tool, the authors reviewed and  
556 edited the content as needed and take full responsibility for the content of the  
557 publication.

558

### 559 **Data Availability Statement**

560 Full summary statistics for the gwas study of SSHS can be accessed from  
561 <https://figshare.com/> (DOI: 10.6084/m9.figshare.20033246) and Bio-X institutes  
562 website (<http://analysis.bio-x.cn/gwas/>). The raw genetic data for each individual from  
563 our analyses could also be accessed under the Data Access Agreement  
564 (<https://figshare.com/>, DOI: 10.6084/m9.figshare.20033243 and  
565 <http://galaxy.bio-x.cn/library/list#folders/Ff2db41e1fa331b3e>). Additional raw data  
566 can be obtained upon request from the authors.

567

568

### 569 **Acknowledgements**

570 We would like to thank Professor Junli Liu from Shanghai Diabetes Institute,  
571 Department of Endocrinology and Metabolism, Shanghai Jiao Tong University  
572 Affiliated Sixth People's Hospital for his assistance in indirect experiment. This study  
573 was also supported by grants-in-aid from Ministry of Science and Technology of the  
574 People' s Republic of China (2021ZD0201900), National Natural Science Foundation  
575 of China (81971240, 82070824, 82171125, 81970869, 81970870, 82271153,  
576 82000967, 82101205, 82100105, 82301291, 82300962), Shanghai Municipal  
577 Commission of Science and Technology (Grant No.18DZ2260200), the  
578 Interdisciplinary Program of Shanghai Jiao Tong University (YG2023LC11), Youth  
579 Innovation Promotion Association of CAS (2023289), Shanghai Sailing Program  
580 grant (23YF1431900). The funding sources had no role in design, conduct, analysed,  
581 and interpreted of this study.

## 582 **Appendix Supplementary data**

583 Supplementary Figures

584 Supplementary Context

585 Supplementary Materials

## 586 **References**

587 [1]. Åberg, F., et al., Alcohol consumption and metabolic syndrome: Clinical and  
588 epidemiological impact on liver disease. *J Hepatol*, 2023. 78(1): p. 191-206. DOI:  
589 10.1016/j.jhep.2022.08.030.

590

591 [2]. Mesarwi, O.A., R. Loomba, and A. Malhotra, Obstructive Sleep Apnea, Hypoxia,  
592 and Nonalcoholic Fatty Liver Disease. *Am J Respir Crit Care Med*, 2019. 199(7): p.  
593 830-841. DOI: 10.1164/rccm.201806-1109TR.

594

595 [3]. Gaines, J., et al., Obstructive sleep apnea and the metabolic syndrome: The road  
596 to clinically-meaningful phenotyping, improved prognosis, and personalized  
597 treatment. *Sleep Med Rev*, 2018. 42: p. 211-219. DOI: 10.1016/j.smrv.2018.08.009.

598

599 [4]. Xu, S., et al., The association between obstructive sleep apnea and metabolic  
600 syndrome: a systematic review and meta-analysis. *BMC Pulm Med*, 2015. 15: p. 105.  
601 DOI: 10.1186/s12890-015-0102-3.

602

- 603 [5]. Trzepizur, W., et al., Sleep Apnea-Specific Hypoxic Burden, Symptom Subtypes,  
604 and Risk of Cardiovascular Events and All-Cause Mortality. *Am J Respir Crit Care*  
605 *Med*, 2022. 205(1): p. 108-117. DOI: 10.1164/rccm.202105-1274OC.
- 606
- 607 [6]. Guo, C., et al., ANGPTL8 in metabolic homeostasis: more friend than foe? *Open*  
608 *Biol*, 2021. 11(9): p. 210106. DOI: 10.1098/rsob.210106.
- 609
- 610 [7]. Zhang, R. and A.B. Abou-Samra, Emerging roles of Lipasin as a critical lipid  
611 regulator. *Biochem Biophys Res Commun*, 2013. 432(3): p. 401-5. DOI:  
612 10.1016/j.bbrc.2013.01.129.
- 613
- 614 [8]. Meng, M., et al., Zinc finger protein ZNF638 regulates triglyceride metabolism  
615 via ANGPTL8 in an estrogen dependent manner. *Metabolism*, 2024. 152: p. 155784.  
616 DOI: 10.1016/j.metabol.2024.155784.
- 617
- 618 [9]. Guo, T., et al., Association of the angiotensin-like protein 8 rs2278426  
619 polymorphism and several environmental factors with serum lipid levels. *Mol Med*  
620 *Rep*, 2015. 12(3): p. 3285-3296. DOI: 10.3892/mmr.2015.3825.
- 621
- 622 [10]. Crujeiras, A.B., et al., Interplay of atherogenic factors, protein intake and  
623 betatrophin levels in obese-metabolic syndrome patients treated with hypocaloric  
624 diets. *Int J Obes (Lond)*, 2016. 40(3): p. 403-10. DOI: 10.1038/ijo.2015.206.
- 625
- 626 [11]. Luo, M. and D. Peng, ANGPTL8: An Important Regulator in Metabolic  
627 Disorders. *Front Endocrinol (Lausanne)*, 2018. 9: p. 169. DOI:  
628 10.3389/fendo.2018.00169.
- 629
- 630 [12]. Wang, D., et al., Angiotensin-Like Protein 8/Leptin Crosstalk Influences  
631 Cardiac Mass in Youths With Cardiometabolic Risk: The BCAMS Study. *Front*  
632 *Endocrinol (Lausanne)*, 2021. 12: p. 788549. DOI: 10.3389/fendo.2021.788549.
- 633
- 634 [13]. Chen, X., et al., Circulating betatrophin levels are increased in patients with type  
635 2 diabetes and associated with insulin resistance. *J Clin Endocrinol Metab*, 2015.  
636 100(1): p. E96-100. DOI: 10.1210/jc.2014-2300.
- 637
- 638 [14]. Al-Terki, A., et al., Increased Level of Angiotensin Like Proteins 4 and 8 in  
639 People With Sleep Apnea. *Front Endocrinol (Lausanne)*, 2018. 9: p. 651. DOI:  
640 10.3389/fendo.2018.00651.
- 641
- 642 [15]. Song, Z., et al., Decreased serum betatrophin may correlate with the  
643 improvement of obstructive sleep apnea after Roux-en-Y Gastric Bypass surgery. *Sci*  
644 *Rep*, 2021. 11(1): p. 1808. DOI: 10.1038/s41598-021-81379-1.
- 645
- 646 [16]. Zhang, Z., et al., ANGPTL8 accelerates liver fibrosis mediated by HFD-induced

- 647 inflammatory activity via LILRB2/ERK signaling pathways. *J Adv Res*, 2023. 47: p.  
648 41-56. DOI: 10.1016/j.jare.2022.08.006.
- 649
- 650 [17]. Lee, Y.H., et al., Association between betatrophin/ANGPTL8 and non-alcoholic  
651 fatty liver disease: animal and human studies. *Sci Rep*, 2016. 6: p. 24013. DOI:  
652 10.1038/srep24013.
- 653
- 654 [18]. Chen, J., et al., In vivo targeted delivery of ANGPTL8 gene for beta cell  
655 regeneration in rats. *Diabetologia*, 2015. 58(5): p. 1036-44. DOI:  
656 10.1007/s00125-015-3521-z.
- 657
- 658 [19]. DiDonna, N.M., Y.Q. Chen, and R.J. Konrad, Angiotensin-like proteins and  
659 postprandial partitioning of fatty acids. *Curr Opin Lipidol*, 2022. 33(1): p. 39-46. DOI:  
660 10.1097/MOL.0000000000000798.
- 661
- 662 [20]. Zhang, R. and K. Zhang, An updated ANGPTL3-4-8 model as a mechanism of  
663 triglyceride partitioning between fat and oxidative tissues. *Prog Lipid Res*, 2022. 85: p.  
664 101140. DOI: 10.1016/j.plipres.2021.101140.
- 665
- 666 [21]. Henneman, P., et al., Genetic architecture of plasma adiponectin overlaps with  
667 the genetics of metabolic syndrome-related traits. *Diabetes Care*, 2010. 33(4): p.  
668 908-13. DOI: 10.2337/dc09-1385.
- 669
- 670 [22]. Fall, T. and E. Ingelsson, Genome-wide association studies of obesity and  
671 metabolic syndrome. *Mol Cell Endocrinol*, 2014. 382(1): p. 740-757. DOI:  
672 10.1016/j.mce.2012.08.018.
- 673
- 674 [23]. Aguilera, C.M., J. Olza, and A. Gil, Genetic susceptibility to obesity and  
675 metabolic syndrome in childhood. *Nutr Hosp*, 2013. 28 Suppl 5: p. 44-55. DOI:  
676 10.3305/nh.2013.28.sup5.6917.
- 677
- 678 [24]. Norris, J.M. and S.S. Rich, Genetics of glucose homeostasis: implications for  
679 insulin resistance and metabolic syndrome. *Arterioscler Thromb Vasc Biol*, 2012.  
680 32(9): p. 2091-6. DOI: 10.1161/ATVBAHA.112.255463.
- 681
- 682 [25]. Su, X., Y. Cheng, and B. Wang, ANGPTL8 in cardio-metabolic diseases. *Clin*  
683 *Chim Acta*, 2021. 519: p. 260-266. DOI: 10.1016/j.cca.2021.05.017.
- 684
- 685 [26]. Cannon, M.E., et al., Trans-ancestry Fine Mapping and Molecular Assays  
686 Identify Regulatory Variants at the ANGPTL8 HDL-C GWAS Locus. *G3 (Bethesda)*,  
687 2017. 7(9): p. 3217-3227. DOI: 10.1534/g3.117.300088.
- 688
- 689 [27]. Hanson, R.L., et al., The Arg59Trp variant in ANGPTL8 (betatrophin) is  
690 associated with total and HDL-cholesterol in American Indians and Mexican



- 691 Americans and differentially affects cleavage of ANGPTL3. *Mol Genet Metab*, 2016.  
692 118(2): p. 128-37. DOI: 10.1016/j.ymgme.2016.04.007.  
693
- 694 [28]. Lee, Y.H., et al., APOE and KLF14 genetic variants are sex-specific for low  
695 high-density lipoprotein cholesterol identified by a genome-wide association study.  
696 *Genet Mol Biol*, 2022. 45(1): p. e20210280. DOI:  
697 10.1590/1678-4685-GMB-2021-0280.  
698
- 699 [29]. Quagliarini, F., et al., Atypical angiotensin-like protein that regulates  
700 ANGPTL3. *Proc Natl Acad Sci U S A*, 2012. 109(48): p. 19751-6. DOI:  
701 10.1073/pnas.1217552109.  
702
- 703 [30]. Xu, H., et al., Genome-Wide Association Study of Obstructive Sleep Apnea and  
704 Objective Sleep-related Traits Identifies Novel Risk Loci in Han Chinese Individuals.  
705 *Am J Respir Crit Care Med*, 2022. 206(12): p. 1534-1545. DOI:  
706 10.1164/rccm.202109-2044OC.  
707
- 708 [31]. Funke, B., et al., The mouse poly(C)-binding protein exists in multiple isoforms  
709 and interacts with several RNA-binding proteins. *Nucleic Acids Res*, 1996. 24(19): p.  
710 3821-8. DOI: 10.1093/nar/24.19.3821.  
711
- 712 [32]. Rosenbluh, J., et al., Genetic and Proteomic Interrogation of Lower Confidence  
713 Candidate Genes Reveals Signaling Networks in  $\beta$ -Catenin-Active Cancers. *Cell Syst*,  
714 2016. 3(3): p. 302-316.e4. DOI: 10.1016/j.cels.2016.09.001.  
715
- 716 [33]. Huttlin, E.L., et al., Dual proteome-scale networks reveal cell-specific  
717 remodeling of the human interactome. *Cell*, 2021. 184(11): p. 3022-3040.e28. DOI:  
718 10.1016/j.cell.2021.04.011.  
719
- 720 [34]. Dempsey, J.A., et al., Pathophysiology of sleep apnea. *Physiol Rev*, 2010. 90(1):  
721 p. 47-112. DOI: 10.1152/physrev.00043.2008.  
722
- 723 [35]. Siddle, K., Signalling by insulin and IGF receptors: supporting acts and new  
724 players. *J Mol Endocrinol*, 2011. 47(1): p. R1-10. DOI: 10.1530/JME-11-0022.  
725
- 726 [36]. Alkrekshi, A., et al., A comprehensive review of the functions of YB-1 in cancer  
727 stemness, metastasis and drug resistance. *Cell Signal*, 2021. 85: p. 110073. DOI:  
728 10.1016/j.cellsig.2021.110073.  
729
- 730 [37]. Fu, Y., et al., Meta-analysis of all-cause and cardiovascular mortality in  
731 obstructive sleep apnea with or without continuous positive airway pressure treatment.  
732 *Sleep Breath*, 2017. 21(1): p. 181-189. DOI: 10.1007/s11325-016-1393-1.  
733
- 734 [38]. Framnes, S.N. and D.M. Arble, The Bidirectional Relationship Between

- 735 Obstructive Sleep Apnea and Metabolic Disease. *Front Endocrinol (Lausanne)*, 2018.  
736 9: p. 440. DOI: 10.3389/fendo.2018.00440.  
737
- 738 [39]. Meszaros, M., et al., Obstructive sleep apnea and hypertriglyceridaemia share  
739 common genetic background: Results of a twin study. *J Sleep Res*, 2020. 29(4): p.  
740 e12979. DOI: 10.1111/jsr.12979.  
741
- 742 [40]. Popko, K., et al., Frequency of distribution of leptin receptor gene  
743 polymorphism in obstructive sleep apnea patients. *J Physiol Pharmacol*, 2007. 58  
744 Suppl 5(Pt 2): p. 551-61.  
745
- 746 [41]. Bielicki, P., et al., Impact of polymorphism of selected genes on the diagnosis of  
747 type 2 diabetes in patients with obstructive sleep apnea. *Pol Arch Intern Med*, 2019.  
748 129(1): p. 6-11. DOI: 10.20452/pamw.4406.  
749
- 750 [42]. Chen, S., et al., Angptl8 mediates food-driven resetting of hepatic circadian  
751 clock in mice. *Nat Commun*, 2019. 10(1): p. 3518. DOI:  
752 10.1038/s41467-019-11513-1.  
753
- 754 [43]. Lyabin, D.N., I.A. Eliseeva, and L.P. Ovchinnikov, YB-1 protein: functions and  
755 regulation. *Wiley Interdiscip Rev RNA*, 2014. 5(1): p. 95-110. DOI:  
756 10.1002/wrna.1200.  
757
- 758 [44]. Wolffe, A.P., Structural and functional properties of the evolutionarily ancient  
759 Y-box family of nucleic acid binding proteins. *Bioessays*, 1994. 16(4): p. 245-51. DOI:  
760 10.1002/bies.950160407.  
761
- 762 [45]. Ceman, S., R. Nelson, and S.T. Warren, Identification of mouse YB1/p50 as a  
763 component of the FMRP-associated mRNP particle. *Biochem Biophys Res Commun*,  
764 2000. 279(3): p. 904-8. DOI: 10.1006/bbrc.2000.4035.  
765
- 766 [46]. Rabiee, A., et al., White adipose remodeling during browning in mice involves  
767 YBX1 to drive thermogenic commitment. *Mol Metab*, 2021. 44: p. 101137. DOI:  
768 10.1016/j.molmet.2020.101137.  
769
- 770 [47]. Park, J.H., et al., A multifunctional protein, EWS, is essential for early brown fat  
771 lineage determination. *Dev Cell*, 2013. 26(4): p. 393-404. DOI:  
772 10.1016/j.devcel.2013.07.002.  
773
- 774 [48]. Wu, R., et al., RNA-binding protein YBX1 promotes brown adipogenesis and  
775 thermogenesis via PINK1/PRKN-mediated mitophagy. *Faseb j*, 2022. 36(3): p.  
776 e22219. DOI: 10.1096/fj.202101810RR.  
777
- 778 [49]. Zou, J., et al., Independent relationships between cardinal features of

779 obstructive sleep apnea and glycometabolism: a cross-sectional study. *Metabolism*,  
 780 2018. 85: p. 340-347. DOI: 10.1016/j.metabol.2017.11.021.

781  
 782  
 783  
 784

785 **Table1. Eighteen Genetic variant loci associated with serum CHOL, TRIG, LDL-C and**  
 786 **HDL-C levels in GWAS cohort.**

787

Traits	SNP ID	Chr	A1	A2	$\beta$	SE	$p$ value	MAF
CHOL	rs3832016	1	C	CT	-0.2278	0.03897	$5.34 \times 10^{-09}$	0.05824
CHOL	rs80246393	6	G	A	0.5041	0.0922	$4.76 \times 10^{-08}$	0.01101
TRIG	rs80266524	1	C	A	0.9058	0.1648	$4.06 \times 10^{-08}$	0.01118
TRIG	rs57539228	3	A	G	0.9427	0.1664	$1.54 \times 10^{-08}$	0.01082
TRIG	rs117362525	3	C	T	0.8484	0.1514	$2.22 \times 10^{-08}$	0.01429
TRIG	rs151299191	10	G	A	0.9586	0.1708	$2.09 \times 10^{-08}$	0.01019
TRIG	rs147511495	10	A	G	0.9014	0.1504	$2.16 \times 10^{-09}$	0.01373
TRIG	rs651821	11	C	T	0.5633	0.03756	$6.22 \times 10^{-50}$	0.2807
TRIG	rs34528262	13	T	G	0.9393	0.159	$3.69 \times 10^{-09}$	0.01197
TRIG	rs79929907	16	G	A	0.779	0.1252	$5.26 \times 10^{-10}$	0.01956
TRIG	rs483082	19	T	G	0.2837	0.04654	$1.16 \times 10^{-09}$	0.1889
LDL-C	rs12740374	1	T	G	-0.1934	0.03203	$1.68 \times 10^{-09}$	0.05762
LDL-C	rs72654473	19	A	C	-0.3973	0.02821	$2.73 \times 10^{-44}$	0.07703
HDL-C	rs115849089	8	A	G	0.04752	0.006862	$4.81 \times 10^{-12}$	0.1127
HDL-C	rs651821	11	C	T	-0.04699	0.004766	$9.34 \times 10^{-23}$	0.2807

HDL-C	rs12149545	16	A	G	0.05475	0.005868	$1.45 \times 10^{-20}$	0.1616
HDL-C	rs3786247	18	G	T	0.02829	0.004447	$2.17 \times 10^{-10}$	0.4083
HDL-C	rs3745683	19	A	G	-0.0316	0.004896	$1.18 \times 10^{-10}$	0.2695

788

789

790 A1, minor allele; A2, major allele; MAF, minor allele frequency.

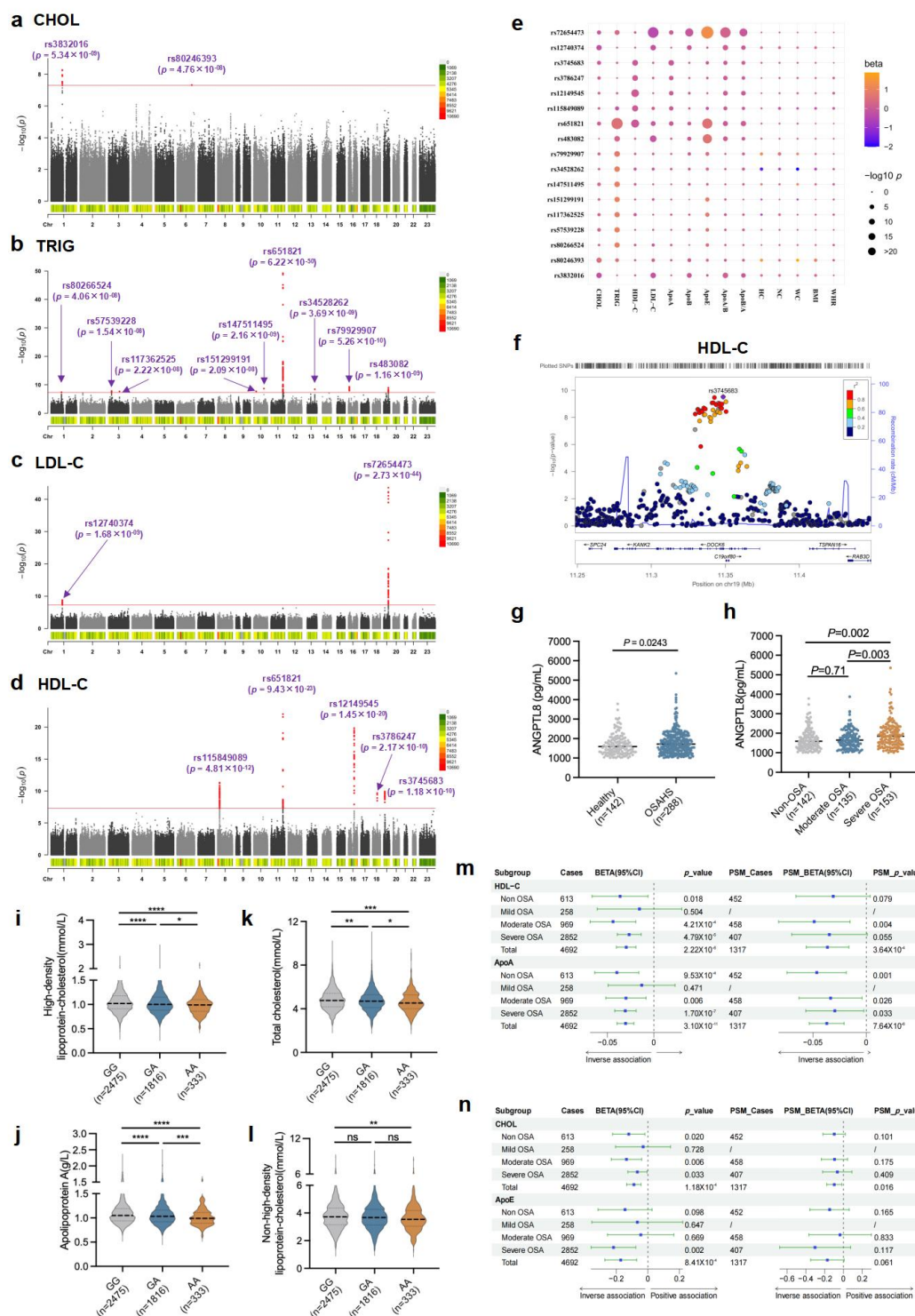
791

792

793

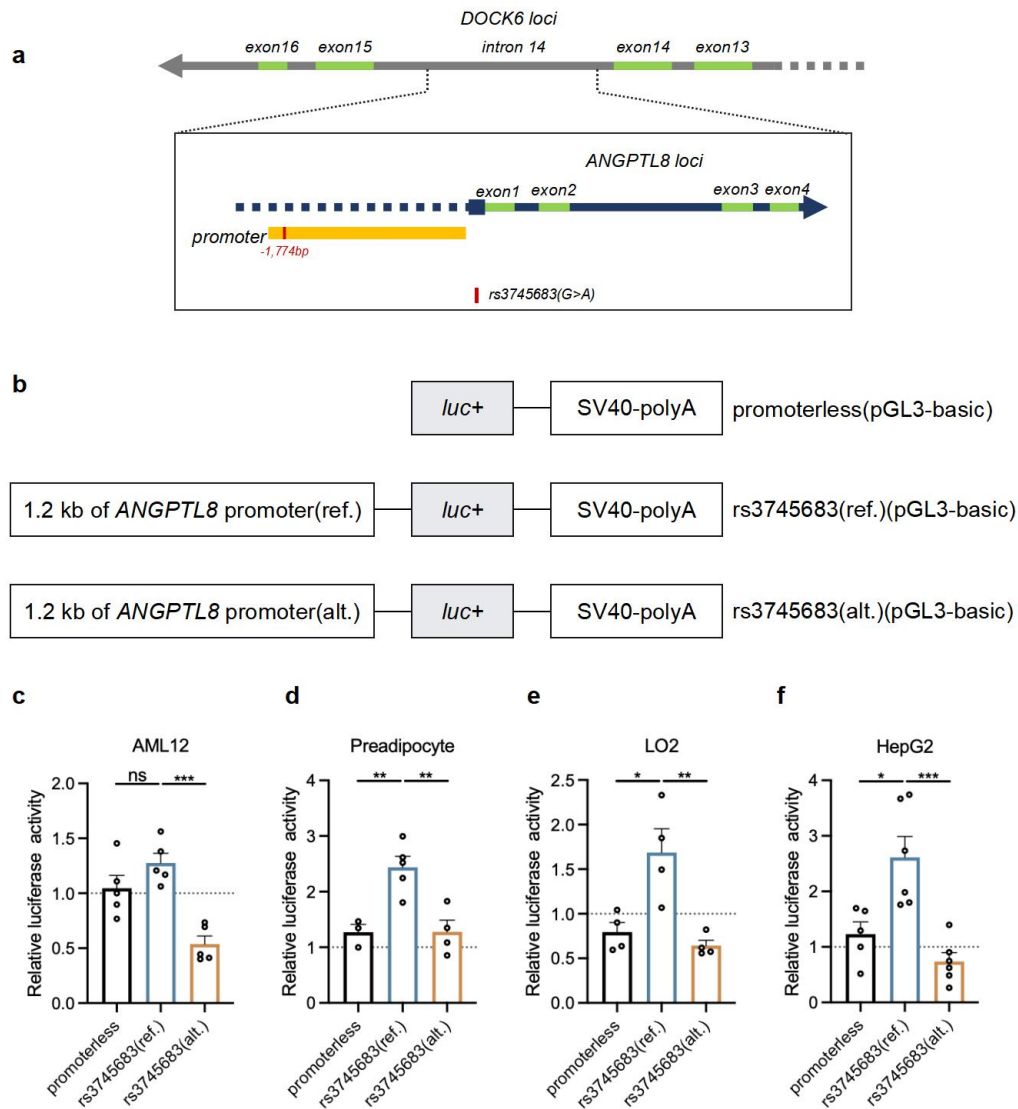
## 794 **Figures**

795 **Figure 1 GWAS identified novel genetic loci associated with serum lipid traits in**  
796 **Han Chinese OSA patients. (a-d)** Manhattan plot showing the genome-wide  $p$   
797 values of association with serum CHOL **(a)**, TRIG **(b)**, LDL-C **(c)**, and HDL-C **(d)**.  
798 The red line shows the genome-wide significant threshold of  $p < 5 \times 10^{-8}$ . **(e)** Dotplot  
799 presents the associations between indicated variants and the quantitative traits. **(f)**  
800 Region plot of association between rs3745683 and HDL-C. The purple dot indicates  
801 rs3745683. **(g, h)** Serum ANGPTL8 levels in OSA patients. **(i-l)** The comparison of  
802 serum HDL-C **(i)**, CHOL **(k)**, ApoA **(j)**, and non HDL-C **(l)** levels among three  
803 genotypes of rs3745683. \* $p < 0.05$ , \*\* $p < 0.01$ , \*\*\* $p < 0.001$ , \*\*\*\* $p < 0.0001$ . **(m, n)**  
804 Effects of rs3745683(G>A) on serum HDL-C **(m)**, ApoA **(m)**, CHOL **(n)**, and ApoE  
805 **(n)** among different severity OSA patients. Beta and  $p$  value were obtained by linear  
806 regression analysis with or without adjusting for age, gender, cigarette consumption,  
807 and alcohol consumption.



808

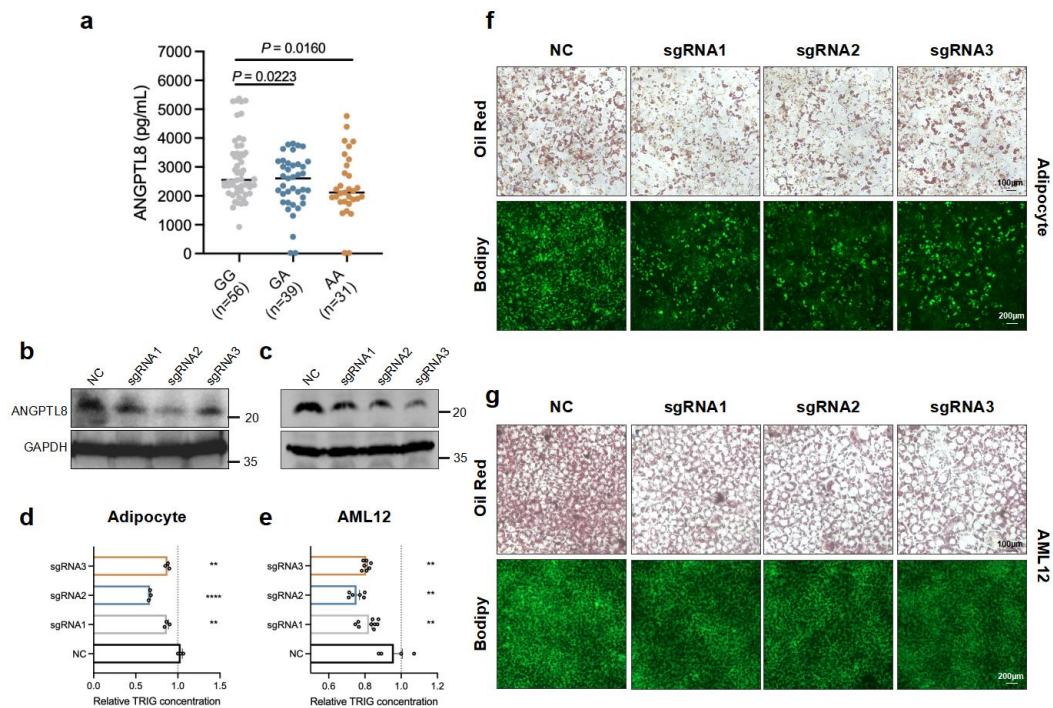
809 **Figure 2 rs3745683 suppressed transcriptional activity of ANGPTL8 promoter.**  
 810 (a) Diagram of rs3745683 in ANGPTL8 promoter. (b) Scheme of vector constructs.  
 811 (c-f) Mean (sem) transcriptional activity of ANGPTL8 promoter with reference allele  
 812 (G) or alternative allele (A) in AML12 (c), mouse preadipocytes (d), LO2 (e), and  
 813 HepG2 (f) cells. The y axis represents the relative luciferase activity.



814

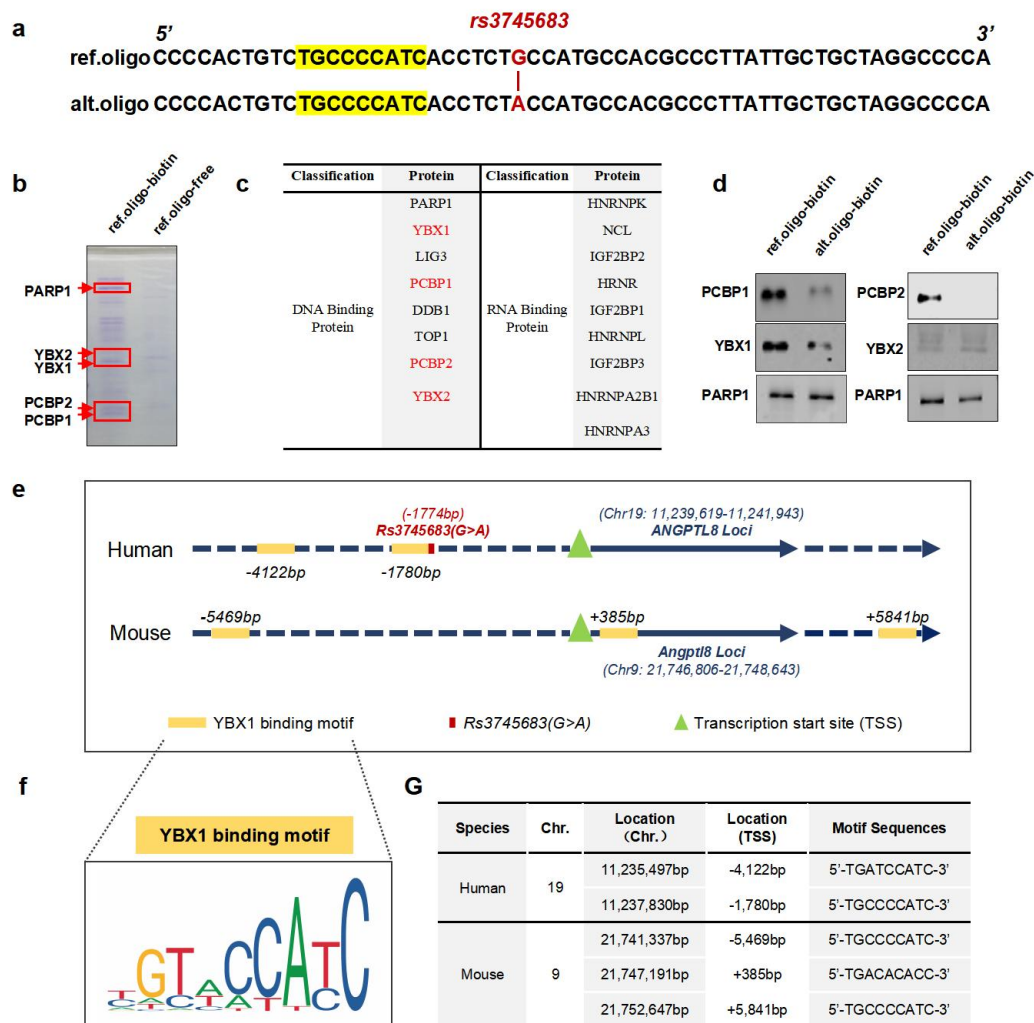
815 **Figure 3 An essential role of ANGPTL8 in lipogenesis.** (a) The comparison of  
 816 serum ANGPTL8 level among three genotypes of rs3745683. (b, c) Protein levels of  
 817 ANGPTL8 in *Angptl8*-sgRNA transfected adipocytes (b) and AML12 cells (c). (d)  
 818 Triglyceride content analysis of *Angptl8*-sgRNA transfected adipocytes differentiated  
 819 for 6 days. (e) Triglyceride content analysis of *Angptl8*-sgRNA transfected AML12

820 cells differentiated for 1 day. **(f)** Oil red staining and Bodipy 493/503 dye staining of  
 821 *Angptl8*-sgRNA transfected adipocytes differentiated for 6 days. **(g)** Oil red staining  
 822 and Bodipy 493/503 dye staining of *Angptl8*-sgRNA transfected AML12 cells  
 823 differentiated for 1 day.



825 **Figure 4 Identification of YBX1 as a transcriptional factor of rs3745683 proximal**  
826 **region. (a)** DNA probe sequences containing rs3745683(G>A) locus. Highlight  
827 indicates the predicted YBX1 DNA binding motif. **(b)** Coomassie brilliant  
828 blue-stained acrylamide gel of a pulldown assay using oligonucleotides containing  
829 allele G of rs3745683. **(c)** Selected proteins in the ref.oligo-biotin precipitate  
830 identified by LC-MS analysis. **(d)** Immunoblots of a pulldown assay using  
831 oligonucleotides containing either allele G and A of rs3745683. **(e, g)** Predicted YBX1  
832 DNA binding Motif in *ANGPTL8* gene among human and mouse. **(f)** Motif analysis  
833 of YBX1-bound sequence, available at <https://jaspar.elixir.no/matrix/UN0139.1/>.

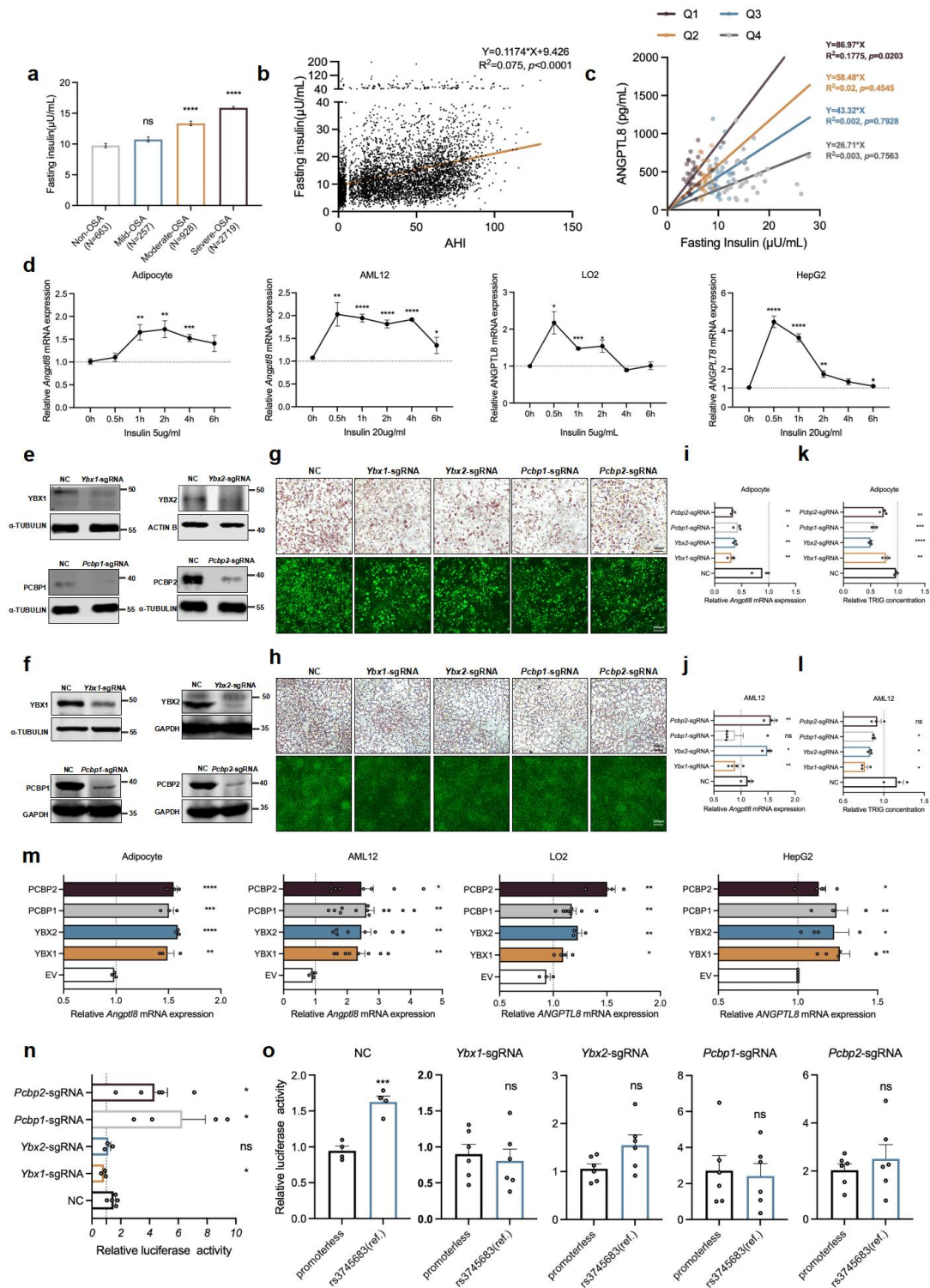




834

835 **Figure 5 Effects of YYP on Angptl8 expression and lipid metabolism. (a-b)**  
 836 Fasting insulin level in OSA patients (a) and correlation between insulin level and  
 837 AHI (b). (c) Linear association analysis of serum ANGPTL8 and fasting insulin level  
 838 in different HOMA-IR group. (d) *ANGPTL8* mRNA levels in mouse adipocytes,  
 839 AML12, LO2, and HepG2 cells following the stimulation of insulin over a 6-h period.

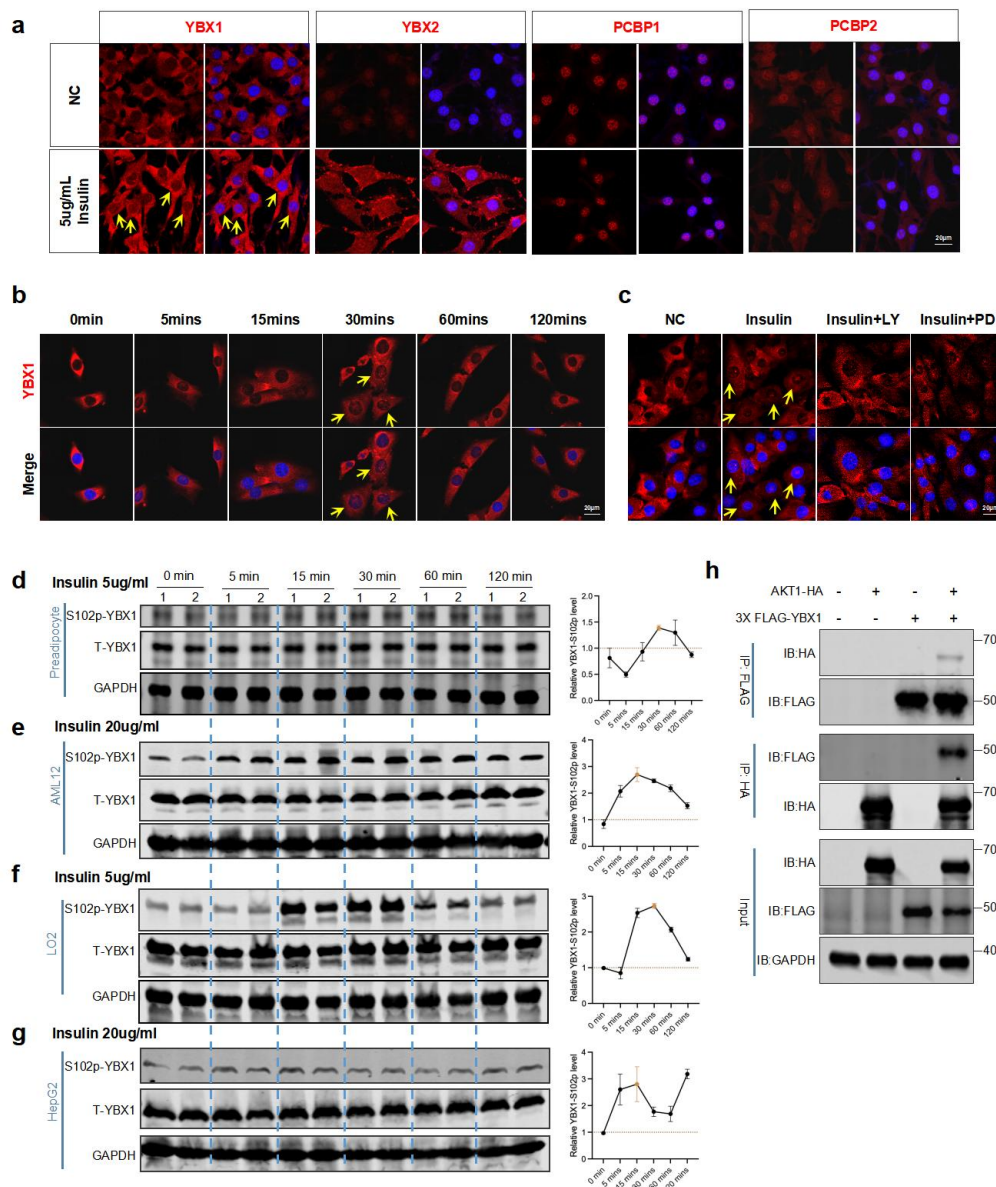
840 **(e-f)** Immunoblots of YYPP-sgRNA knockout efficiency in mouse preadipocytes **(e)**  
841 and AML12 cells **(f)**. **(g-h)** Oil red staining and Bodipy 493/503 dye staining in  
842 YYPP-sgRNAs transfected adipocytes differentiated for 6 days **(g)**, and AML12 cells  
843 200uM PA treated for 1 day **(h)**. **(i-j)** *Angptl8* mRNA levels in YYPP-sgRNAs  
844 transfected mouse adipocytes differentiated for 6 days **(i)**, and AML12 cells 200uM  
845 PA treated for 1 day **(j)**. **(k-l)** TRIG content in YYPP-sgRNAs transfected mouse  
846 adipocytes differentiated for 6 days **(k)**, and AML12 cells 200uM PA treated for 1 day  
847 **(l)**. **(m)** *ANGPTL8* mRNA levels in mouse adipocytes, AML12, LO2, and HepG2  
848 cells after overexpression MYC-tagged YYPP for 2 days. **(n)** Mean (sem)  
849 transcriptional activity of *ANGPTL8* promoter with reference allele in YYPP  
850 deficiency preadipocytes. **(o)** Transcriptional activity comparison of vector constructs  
851 between promoterless and *ANGPTL8* promoter with reference allele in YYPP  
852 deficiency preadipocytes.



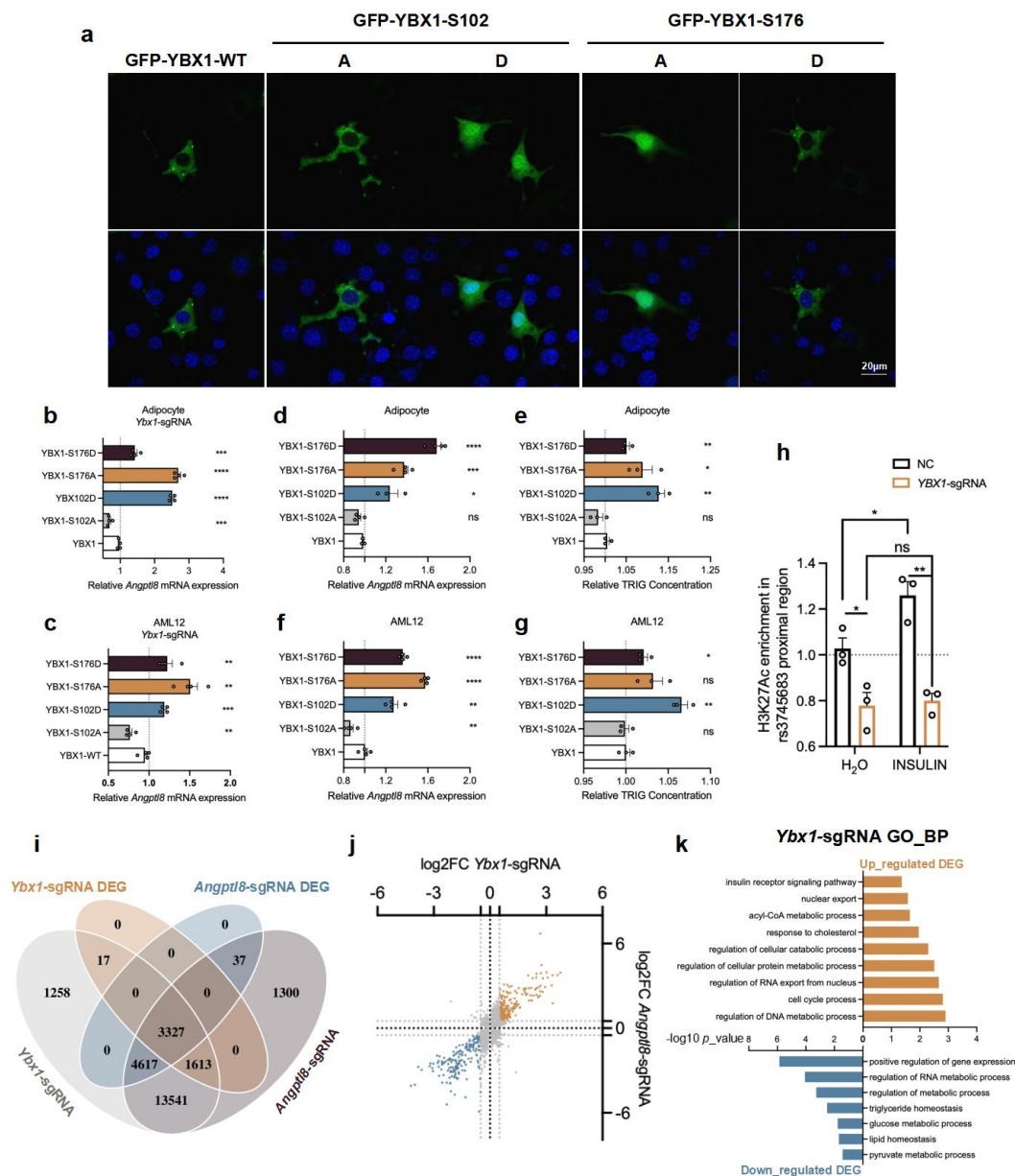
853

854 **Figure 6 Insulin signaling triggers YBX1 phosphorylation and nuclear**  
 855 **translocation through interaction between YBX1 and AKT. (a)** Subcellular  
 856 **localization of YYPP in preadipocytes stimulated by 5 $\mu\text{g/mL}$  insulin for 24 h. (b)**  
 857 **Subcellular localization of YBX1 in preadipocytes following the stimulation of**  
 858 **5 $\mu\text{g/mL}$  insulin over a 2-h period. (c)** Subcellular localization of YBX1 in

859 preadipocytes which stimulated by 5 $\mu$ g/mL insulin, 5 $\mu$ g/mL insulin+20 $\mu$ M LY294002,  
 860 or 5 $\mu$ g/mL insulin+10 $\mu$ M PD98059 for 30mins, respectively. **(d-g)** YBX1-S102p  
 861 levels in mouse preadipocytes **(d)**, AML12 **(e)**, LO2 **(f)**, and HepG2 **(g)** cells  
 862 following the stimulation of insulin over a 2-h period. **(h)** Co-Immunoprecipitation  
 863 analysis of 3 $\times$ FLAG-YBX1 and AKT1-HA.



865 **Figure 7 The phosphorylation dependent nuclear translocation of YBX1**  
866 **promotes ANGPTL8 expression. (a)** Subcellular localization of GFP-tagged YBX1  
867 variations (WT, S102A, S102D, S176A, and S176D) in preadipocytes. The nuclei  
868 were stained with DAPI. These images were captured at 630 magnification. **(b-c)**  
869 *Angptl8* mRNA levels in *Ybx1*-sgRNA transfected mouse adipocytes **(b)**, and AML12  
870 cells **(c)** which overexpressed 5 YBX1 variations respectively. **(d-e)** *Angptl8* mRNA  
871 levels **(d)**, and TRIG content **(e)** in mouse adipocytes which overexpressed 5 YBX1  
872 variations respectively. **(f-g)** *Angptl8* mRNA levels **(f)** and TRIG content **(g)** in  
873 AML12 cells which overexpressed 5 YBX1 variations respectively. **(h)** With or  
874 without 20 $\mu$ g/mL insulin stimulation, H3K27Ac occupancy analysis of rs3745683  
875 proximal region in HepG2 cells by CUT & Tag-qPCR. **(i)** Venn plot of gene  
876 expression profiles in *Ybx1*-sgRNA and *Angptl8*-sgRNA AML12 cells, DEG  
877 thresholds:  $p < 0.05$ . **(j)** DEGs ( $p < 0.05$ ) in *Ybx1*-sgRNA and *Angptl8*-sgRNA  
878 AML12 cells. Gray line represented  $|\log_2\text{FoldChange}| = 0.5$ . **(k)** GO pathway  
879 enrichment analysis for biological process in *Ybx1*-sgRNA AML12 cells, up-regulated  
880 and down-regulated DEG thresholds:  $p < 0.05$ ,  $|\log_2\text{FoldChange}| > 0.5$ .



881

882 **Figure 8 YBX1 regulates ANGPTL8 expression and liver lipid metabolism *in vivo*.**  
 883 **(a)** Pictures of AAV infected livers. **(b-d)** Levels of *Angptl8* mRNA **(b)** and protein  
 884 **(c-d)** in AAV-*Ybx1*-shRNA mouse livers. **(e, f)** Body weights **(e)** and food intake **(f)** of  
 885 AAV-*EV* and AAV-*Ybx1*-shRNA mice. **(g)** Relative tissue weight, fat mass, and lean  
 886 mass of AAV-*EV* and AAV-*Ybx1*-shRNA mice under HFD for 16 weeks. **(h)** Glucose

887 tolerance test of mice under HFD for 12 weeks. **(i- j)** TRIG **(i)** and CHOL **(j)** levels in  
888 serum and liver of AAV-*EV* and AAV-*Ybx1*-shRNA mice. **(k)** Oil red staining of  
889 mouse livers under HFD for 16 weeks. **(l)** Volcano plot showing the DEGs with  
890 statistical significance (thresholds:  $p < 0.05$ ) and fold change (thresholds:  
891  $|\log_2\text{FoldChange}| \geq 1$ ) in the livers of AAV-*EV* and AAV-*Ybx1*-shRNA mice. **(m)** GO  
892 pathway enrichment analysis for biological process in the livers of AAV-*Ybx1*-shRNA  
893 mice, up-regulated and down-regulated DEG thresholds:  $p < 0.05$ ,  $|\log_2\text{FoldChange}| >$   
894 1. **(n-p)** Region plot of association between YBX1 locus **(n)**, YBX2 locus **(o)** and  
895 PCBP1 locus **(p)**, and CHOL trait.

